

Learning Contrastive Feature Representations for Facial Action Unit Detection

Ziqiao Shang , Bin Liu* , Fengmao Lv , Fei Teng , Tianrui Li , *Senior Member, IEEE*

Abstract—Facial action unit (AU) detection has long encountered the challenge of detecting subtle feature differences when AUs activate. Existing methods often rely on encoding pixel-level information of AUs, which not only encodes additional redundant information but also leads to increased model complexity and limited generalizability. Additionally, the accuracy of AU detection is negatively impacted by the class imbalance issue of each AU type, and the presence of noisy and false AU labels. In this paper, we introduce a novel contrastive learning framework aimed for AU detection that incorporates both self-supervised and supervised signals, thereby enhancing the learning of discriminative features for accurate AU detection. To tackle the class imbalance issue, we employ a negative sample re-weighting strategy that adjusts the step size of updating parameters for minority and majority class samples. Moreover, to address the challenges posed by noisy and false AU labels, we employ a sampling technique that encompasses three distinct types of positive sample pairs. This enables us to inject self-supervised signals into the supervised signal, effectively mitigating the adverse effects of noisy labels. Our experimental assessments, conducted on four widely-utilized benchmark datasets (BP4D, DISFA, GFT and Aff-Wild2), underscore the superior performance of our approach compared to state-of-the-art methods of AU detection. Our code is available at <https://github.com/Ziqiao-Shang/AUNCE>.

Index Terms—Facial action unit detection, Contrastive learning, Positive sample sampling, Importance re-weighting strategy.

I. INTRODUCTION

Facial Action Coding System (FACS) [1] is a widely employed approach for facial expression coding, which introduced a set of 44 facial action units (AUs) that establish a link between facial muscle movements and facial expressions [2]. AU detection is a multi-label binary classification problem. Each AU represents a kind of label, and activated and inactivated AUs are respectively labeled 1 and 0. Nowadays, AU detection [3]–[9] has emerged as a computer vision technique to automatically identify AUs in videos or images. This advancement holds promise for diverse applications, including human-computer interaction [10], emotion analysis [11], [12], and car driving monitoring [13].

In recent years, there has been a prevailing trend in supervised frameworks for AU detection [14]–[20]. These studies have predominantly utilized the binary cross-entropy loss to

Ziqiao Shang is with the School of Electronic Information and Communications, Huazhong University of Science and Technology, Wuhan 430074, China (e-mail: ziqiaosh@gmail.com).

Bin Liu, Fengmao Lv, Fei Teng and Tianrui Li are with the School of Computing and Artificial Intelligence, Southwest Jiaotong University, Chengdu, 610031, China (e-mail: binliu@swjtu.edu.cn; fengmaolv@126.com; fteng@swjtu.edu.cn; trli@swjtu.edu.cn).

*Corresponding author (Bin Liu).

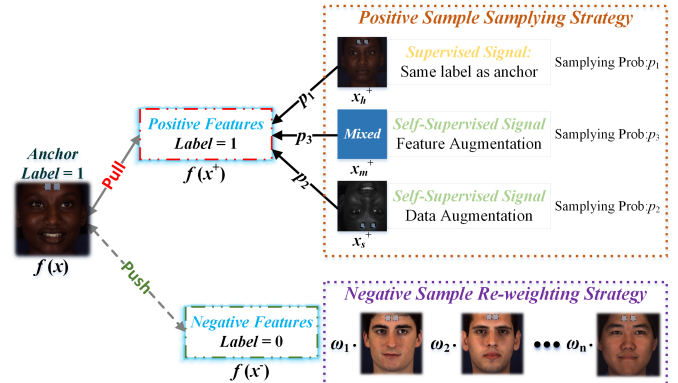


Fig. 1. Overview of our proposed contrastive learning framework.

strictly align predicted and ground truth labels, which is often unnecessary for classification tasks. This overemphasis on label alignment imposes excessive demands on the fitting capacity of models, consequently increasing the risk of overfitting. Moreover, these methods commonly focus on encoding entire pixel-level information of AUs, disregarding the fact that capturing subtle feature differences when AUs activate is sufficient. As a result, these learning methods place significant demands on the model complexity to encode excessive redundant information, ultimately limiting the generalization ability of the model.

Representation learning approaches rooted in contrastive learning have demonstrated substantial promise [21]–[25] for classification. This approach aims to maximize the consistency of positive samples that are semantically similar while minimizing the consistency of negative samples that are semantically dissimilar [26]. By optimizing the contrastive loss, the mutual information between variables is either explicitly or implicitly optimized [27]. However, the direct integration of contrastive learning into AU detection encounters two principal challenges. The first challenge is the class imbalance issue of each AU type [14]. Most AU classes manifest a substantial imbalance between majority and minority class samples, with inactivated AUs vastly outnumbering their activated counterparts. This imbalance issue influences the classification decision threshold, potentially resulting in the direct classification of the majority of AUs as the negative class. The second challenge pertains to the noisy and false label problem [28]. Due to the subtle feature differences when AUs activate leading to the inherent difficulty in expertly labeling AUs, existing AU datasets may exhibit a few noisy and false labels, significantly undermining the overall fitting

ability of models.

To address these challenges, we propose a contrastive learning framework designed to encode discriminative features for AU detection, as depicted in Fig. 1. This approach serves as a replacement for traditional pixel-level learning methods, which also offers a pathway to the lightweight model development within the field of AU detection. The resultant loss is termed AUNCE, resembling the commonly utilized InfoNCE. Moreover, to mitigate the class imbalance issue of each AU type, we apply a negative sample re-weighting strategy, making modifications to the gradient magnitude of minority and majority class samples during back-propagation by adding importance weight to the denominator of the resultant loss. Additionally, in response to the issue of noisy and false labeling in AUs, we introduce a positive sample sampling strategy to augment the supervision signal through self-supervised signals. This is achieved by establishing sampling ratios for various types of positive sample pairs, ensuring that more robust positive samples are derived from data augmentation with the self-supervised signal. The primary contributions of our work are succinctly summarized as follows:

- We propose a contrastive learning framework to learn discriminative feature representations for AU detection, and the resultant loss is named AUNCE.
- We employ a negative sample re-weighting strategy to tackle the class imbalance issue of each AU type.
- We introduce a positive sample sampling strategy to address the issue of noisy and false AU labels.
- We validate the effectiveness of AUNCE by comparing it to state-of-the-art approaches for AU detection on four widely-used datasets, namely BP4D, DISFA, GFT and Aff-Wild2.

II. RELATED WORK

We provide a comprehensive overview of two areas closely connected to our research: deep contrastive learning and contrastive learning for AU detection.

A. Deep contrastive learning

Contrastive learning [29] initially emerged from the realm of self-supervised learning, where the self-supervised learning objectives were defined by assigning tasks to agents. Specifically, this approach encompasses the application of diverse image augmentations to identical images, followed by an assessment of the resultant images and their associated features to determine similarity. The primary objective is to augment the similarity among features extracted from the same image while concurrently attenuating the similarity between features derived from distinct images. Subsequently, the evolution of this technology has led to the extension of contrastive learning to supervised and semi-supervised learning paradigms, wherein the utilization of labeled data is leveraged to enhance the representations of model features.

In recent years, discriminative contrastive learning, a subset of deep self-supervised learning methods [30], has witnessed substantial progress. This approach adheres to the learn-to-compare paradigm [31], wherein a distinction is made between

observed data and noisy or erroneous data, preventing the model from engaging in the reconstruction of pixel-level information. Prominent frameworks in this domain include SimCLR by Chen *et al.* [26], which introduces a base encoder network and a projection head trained to maximize agreement utilizing a contrastive loss. Additionally, MoCo, proposed by He *et al.* [32], employs a momentum network to maintain a queue of negative samples for efficient contrastive learning. Seyfi *et al.* [33] and Zhao *et al.* [34] have both proposed improved contrastive learning frameworks based on MoCo. Chen and He [35] mitigate undesired collapsing solutions, eschewing the use of negative sample pairs through a stop-gradient operation. Despite variations and errors in representation encoders (denoted as f) and similarity measures across different tasks [36], [37], the underlying concept remains consistent: training the representation encoder f by optimizing a contrastive loss [38], achieved through contrasting similar pairs (x, x^+) and dissimilar pairs (x, x^-) .

Apart from that, deep contrastive learning not only facilitates the automated extraction of refined feature representations through the comparison of positive and negative sample pairs but also incorporates diverse contrastive losses for optimization. For example, Oord *et al.* [27] optimized feature extraction networks by maximizing consistency between predicted and actual outcomes of sequence data, introducing the widely-utilized InfoNCE loss, which implicitly or explicitly serves as a lower bound for mutual information. Theoretical analyses concerning the generalization bounds of contrastive learning for classification tasks have been provided by Arora *et al.* [39]. Khosla *et al.* [40] extended the contrastive learning concept to supervised settings with a supervised contrastive learning loss, aiming to enhance feature expression using labeled data. Additionally, Chen *et al.* [41] proposed a semi-supervised contrastive learning algorithm, initially pretraining all data through contrastive learning and subsequently transferring knowledge to new models via distillation learning with the aid of labeled data.

There is a discernible shift in the construction of sample pairs for contrastive learning. In cases where data is labeled or partially labeled, positive samples can be constructed using images belonging to the same category, rather than being confined to identical images. This approach augments the diversity of positive sample pairs, consequently enhancing feature expression. Furthermore, contrastive learning serves as a precursor to supervised learning, enabling model pretraining to significantly enhance the performance of subsequent supervised learning models.

B. Contrastive learning for AU detection

Contrastive learning was firstly designed as a pretext task [32] for unsupervised or self-supervised learning and was introduced to the domain of AU detection with limited annotations [42]–[46]. For example, Niu *et al.* [42] introduced a semi-supervised co-training approach that utilized contrastive loss to enforce conditional independence between facial representations generated by two Deep Neural Networks (DNNs). Liu *et al.* [45] introduced a semi-supervised contrastive learning

strategy that concurrently combined region learning, contrastive learning, and pseudo-labeling. Additionally, Chang *et al.* [46] present a knowledge-driven representation learning framework aimed for AU detection, incorporating a contrastive learning module that leverages dissimilarities among facial regions to effectively train the feature encoder.

Subsequent research endeavors extended contrastive learning to supervised settings, aiming at enhancing feature representation for AU detection through the utilization of labeled data [47]–[49]. For example, Wu *et al.* [47] introduced a contrastive feature learning method, enabling a Convolutional Neural Network (CNN) to acquire distinctive features that represent differences between neutral and AU-activated facial images. Chen *et al.* [49] introduced a supervised hierarchical contrastive learning method (SupHCL) aimed at enhancing AU detection by fostering knowledge consistency across distinct facial images and various AUs. In a similar vein, Suresh *et al.* [48] proposed a feature-based positive matching contrastive loss, which facilitates learning distances between positives based on the similarity of corresponding AU embeddings.

Different from the above static image-based approaches, some methods predominantly seek to generalize similarity learning between video frames within the discriminative paradigm [50]–[55]. One of the most representative methods is Li *et al.* [28] proposed, which have capitalized on these attributes by formulating a contrastive self-supervised learning method to encode discriminative AU representations from extensive amounts of unlabeled facial videos.

In summary, contrastive learning has demonstrated promising results in various tasks. However, its direct application to the task of detecting subtle feature differences when AUs activate presents challenges: noisy and erroneous annotations, class imbalance in AUs, and difficulty in distinguishing hard negative samples.

III. METHOD

In Section III, we present a contrastive learning framework specifically designed for the task of AU detection, aiming to incentivize the encoder to learn differential information between AUs from each sample pair, rather than focusing on pixel-level information. Subsequently, we confront two additional challenges: 1. Tackling the issue of class imbalance pertaining to each AU type in order to enhance the accuracy of our framework. 2. Addressing the problem of noisy and false labels, aiming to bolster the robustness of our models against erroneously annotated data.

A. Contrastive learning framework

For the task of AU detection, which falls under the category of multi-label binary classification, the prevalent approach for training models has been the utilization of cross-entropy loss. This loss function measures the disparity between predicted labels and ground truth labels. However, there exists variability in the occurrence rates of different AUs, with some AUs exhibiting low occurrence rates while others display high occurrence rates. Consequently, in contrast to the conventional

cross-entropy loss, we employ a weighted cross-entropy loss [14] denoted as L_{wce}

$$L_{wce} = -\frac{1}{n_{au}} \sum_{i=1}^{n_{au}} w_i [y_i \log \hat{y}_i + (1 - y_i) \log(1 - \hat{y}_i)], \quad (1)$$

where y_i denotes the ground truth value of occurrence (*i.e.*, 0 or 1) of the i -th AU, and \hat{y}_i is the corresponding predicted occurrence probability. This loss effectively guides the training process, encouraging the model to allocate higher probabilities to the correct class labels and lower probabilities to incorrect ones. $w_i = \frac{(1/r_i)n_{au}}{\sum_{i=1}^{n_{au}} (1/r_i)}$ is the weight of the i -th AU determined by its occurrence frequency for balanced training. It permits reducing the impact of loss values associated with those AUs that are more commonly activated in the training set. r_i represents the occurrence frequency of the i -th AU, and n_{au} is the total number of AUs.

However, the classification methods based on cross-entropy loss suffer from a common issue of being overly constrained, which can lead to overfitting and limited generalization. This constraint becomes particularly problematic in the context of AU detection, where different AUs share a common encoder. For each AU of every sample, the predicted output \hat{y} must satisfy the aforementioned condition, placing a significant burden on the fitting capability of the encoder. To address this challenge, we introduce a contrastive learning framework for AU detection. As shown in Fig. 1. It comprises a positive sample mining module that integrates self-supervised signals with supervised signals, aiming to address the issue of noisy labels resulting from subtle differences in AUs. Additionally, a negative sample weighting module is included to tackle class imbalance and hard negative sample mining challenges. These modules will be discussed in detail in Sections III-B and III-C, respectively. The resultant loss is formulated as:

$$\mathcal{L}_{aunce} = \mathbb{E}_{\substack{x \sim p_d \\ x^+ \sim p^+ \\ x^- \sim p^-}} \left\{ -\frac{1}{n_{au}} \sum_{i=1}^{n_{au}} w_i \left[-\log \frac{\text{sim}(f(x), f(x^+))}{\text{sim}(f(x), f(x^+)) + \sum_{j=1}^N \omega_j \cdot \text{sim}(f(x), f(x_j^-))} \right] \right\}, \quad (2)$$

where $f(\cdot)$ serves as an encoder, mapping the features to a d dimensional vector, represents the feature representation of a specific AU. The positive sample of x , denoted as x^+ , corresponds to samples belonging to the same class as x . Specifically, they are derived from three sources: samples from the same class, data augmentation of the anchor point, and feature augmentation of samples from the same class. x^- represents negative samples of x , which are samples from different classes compared to x . $\text{sim}(f(x), f(x^+))$ measures the similarity between x and its positive example x^+ , while $\text{sim}(f(x), f(x_j^-))$ measures the similarity between the sample and its negative example. The term p_d represents the data distribution, p^+ and p^- respectively denote the class conditional distribution of positive and negative samples of x . Inspired by Eq (1), we introduce w_i in Eq (2) to mitigate the influence of loss values related to commonly activated AUs in the training set. Additionally, we incorporate ω_j to re-weight the significance of each negative sample.

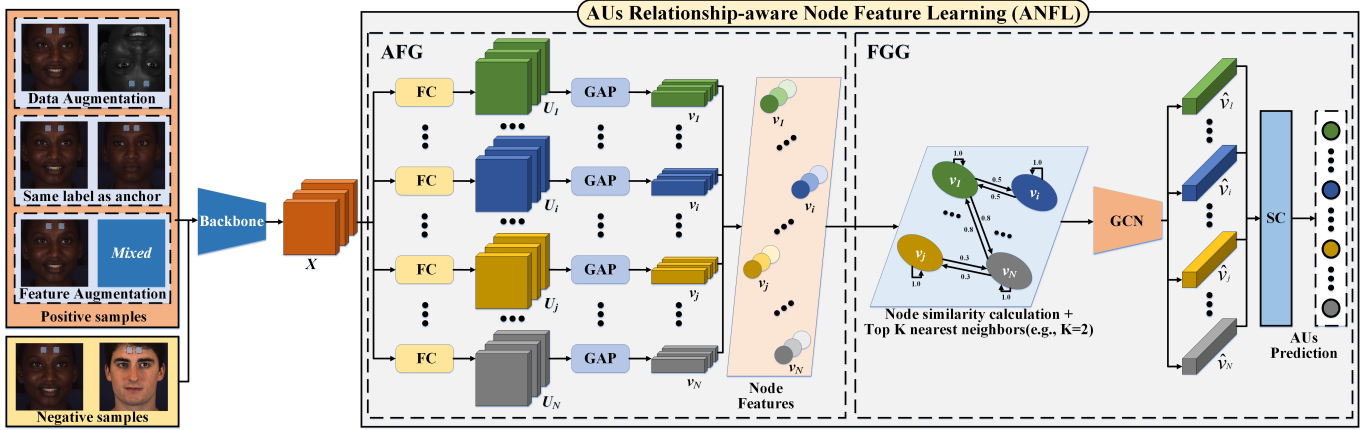


Fig. 2. Overview of the encoder of our contrastive learning framework.

The contrastive loss \mathcal{L}_{aunce} distinguishes itself from weighted cross-entropy loss \mathcal{L}_{wce} in the following aspects: 1. The weighted cross-entropy loss is computed based on the sample and its corresponding label y , requiring the encoding of pixel-level information in order to align with the label. In contrast, the contrastive loss does not involve explicit labels but is computed based on the features of samples from different classes. This incentivizes the encoder to capture the differential information among different class samples, without the need to encode pixel-level information, enabling a lightweight encoder. 2. The weighted cross-entropy loss imposes constraints on the absolute values of the predicted probabilities. However, for classification tasks, this is often unnecessary and can lead to overfitting as well as demanding higher fitting capability from the encoder. The contrastive loss focuses on constraining the similarity difference between positive and negative sample pairs without explicitly specifying their exact values. This is because the minimal value of \mathcal{L}_{aunce} is 0, which is achieved when $\text{sim}(f(x), f(x^+)) - \text{sim}(f(x), f(x_j^-)) \rightarrow +\infty$ for all negative sample index $j \in 1, 2, \dots, N$.

To ensure a fair comparison with conventional pixel-level learning paradigms, we utilize the network structure from the first training stage of MEGraph [56] as our contrastive learning encoder, as illustrated in Fig. 2. The input to the encoder consists of an contrastive learning image pair consisting of an anchor and a random sample, and the encoder is optimized by AUNCE only. Our backbone adopts Swin-transformer [57], and the AUs Relationship-aware Node Feature Learning (ANFL) module is composed of two integral components: the AU-specific Feature Generator (AFG) and the Facial Graph Generator (FGG). The AFG independently generates a unique representation for each AU. Building on these representations, the FGG constructs an optimal graph for each facial display to accurately recognize all target AUs. To accomplish this, the FGG ensures that the AFG encodes task-specific associations among AUs into their respective representations.

B. Negative sample re-weighting strategy

To address the second challenge of the class imbalance issue, we employ a negative sample re-weighting strategy to

minority AUs. This also contributes to hard negative sample mining. Inspired by HCL [58], we apply the following weighting scheme to each negative sample x_j^- :

$$w_j = \text{sim}(f(x), f(x_j^-))^\beta, \quad (3)$$

where $\beta \in (0, +\infty)$ can be viewed as the importance weight if we assume that the negative samples follow a von Mises-Fisher (vMF) distribution. The resulting AUNCE loss is:

$$\mathcal{L}_{aunce} = \mathbb{E}_{\substack{x \sim p_d \\ x^+ \sim p^+ \\ x^- \sim p^-}} \left\{ -\frac{1}{n_{au}} \sum_{i=1}^{n_{au}} w_i \left[-\log \frac{\text{sim}(f(x), f(x^+))}{\text{sim}(f(x), f(x^+)) + \sum_{j=1}^N \text{sim}(f(x), f(x_j^-))^{\beta+1}} \right] \right\}. \quad (4)$$

Next, we analyze how this weighting scheme addresses the class imbalance issue and facilitates the mining of hard negative samples. Without loss of generality, we consider the similarity calculation as $\text{sim}(f(x), f(x^+)) = \exp(f(x)^T f(x^+)/\tau)$, where τ is the temperature coefficient. The inclusion of importance weights transforms the gradient of \mathcal{L} w.r.t similarity scores of positive pairs into the following form:

$$\frac{\partial \mathcal{L}}{\partial \text{sim}(f(x), f(x^+))} = -\frac{1}{\tau} \sum_{j=1}^N P_j, \quad (5)$$

where $P_j = \frac{\exp(f(x)^T f(x_j^-)/\tau)^\beta}{\exp(f(x)^T f(x^+)/\tau) + \sum_{j=1}^N \exp(f(x)^T f(x_j^-)/\tau)^\beta}$, and the gradient of similarity scores of negative pairs $\text{sim}(f(x), f(x^-))$ w.r.t \mathcal{L} is

$$\frac{\partial \mathcal{L}}{\partial \text{sim}(f(x), f(x^-))} = \frac{1}{\tau} P_j. \quad (6)$$

Therefore, the ratio between the gradient magnitude of negative examples and positive examples is given by:

$$\left| \frac{\partial \mathcal{L} / \partial \text{sim}(f(x), f(x^-))}{\partial \mathcal{L} / \partial \text{sim}(f(x), f(x^+))} \right| = \frac{\exp(f(x)^T f(x_j^-)/\tau)^\beta}{\sum_{j=1}^N \exp(f(x)^T f(x_j^-)/\tau)^\beta}. \quad (7)$$

Above equation follows the Boltzmann distribution. As the value of β increases, the entropy of the distribution decreases significantly [59], leading to a sharper distribution in the

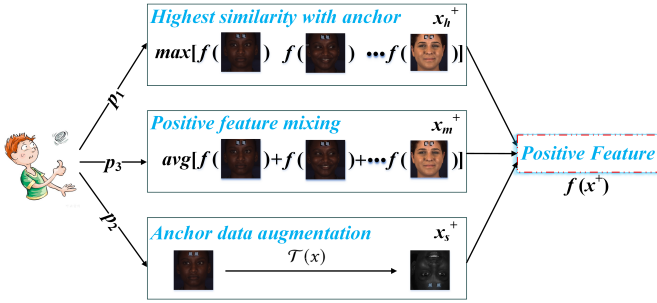


Fig. 3. Illustration of our proposed positive sample sampling strategy.

region of high similarity. This has two consequences: Firstly, it imposes larger penalties on hard negative samples that are in close proximity to the anchor data point, enabling the model to learn more precise decision boundaries from subtle feature differences when AUs activate. Secondly, it controls the relative contribution of negative samples to the parameter updates, providing a means to address class imbalance issues.

Specifically, when anchor data point x belongs to the majority class, its positive sample belongs to the majority class, while its negative sample belongs to the minority class. In this case, we aim to have smaller gradient magnitudes for the positive samples (majority class) to update fewer parameters, while the negative samples (minority class) should have larger gradient magnitudes to update more parameters. To achieve this, we begin to set $\beta \geq 1$, which increases the impact of parameter updates caused by negative samples (minority class). On the other hand, when x belongs to minority class, we begin to set $\beta \leq 1$ to reduce the influence of parameter updates caused by majority class samples. By adjusting the value of β , we can control the relative importance of positive and negative samples during the parameter updating, ensuring that the model pays more attention to minority class samples when necessary and balances the gradient magnitudes accordingly. This helps to balance the representation of different AUs in training set and improves the model ability to precisely classify all AU samples.

C. Positive sample sampling strategy

Regarding the third challenge of AU labels tainted by noise and errors, we employ a combined approach that integrates label noisy learning and self-supervised learning techniques to obtain enhanced supervised signals for positive samples. As shown in Fig. 3, this approach mitigates the adverse effects of noisy labels by simultaneously introducing a controlled level of self-supervised signal and supervised signal, thereby enhancing the robustness of model to variations and errors present in the labeled dataset.

1) *Supervised Signal*: Our supervised signal comes from label noisy learning, which aims to address the issue of mislabeled data by introducing mechanisms that account for label noise during training. One common technique is label smoothing, where a small amount of uncertainty is incorporated into the training process by replacing one-hot labels with smoothed probability distributions. Label smoothing allows

the model to learn from the noisy labels while reducing the negative impact of label errors. However, it is challenging to directly apply label smoothing to contrastive learning as the computation of contrastive loss does not involve explicit labels. To overcome this challenge, we turn to the memory effect of neural networks. Previous research has shown that neural networks tend to first fit clean samples and then memorize the noise in incorrectly labeled samples [60]–[62]. This memory effect is independent of the choice of neural network architecture. The positive samples that are easier fit are those that are closer to the anchor point and have higher similarity. Inspired by this observation, for a given sample x and M positive samples $x_{i=1}^M$ with noisy labels belonging to the same class, we calculate the similarity scores between the representation of sample x and the representations of all M positive samples. We then select the positive feature representation with the highest similarity to sample x :

$$f(x_h^+) = f(x_i), \text{ where } i = \arg \max_i f(x)^T f(x_i). \quad (8)$$

By selecting the positive samples with the highest similarity, we prioritize clean and reliable positive samples while minimizing the influence of noisy positive samples during the training process.

2) *Self-supervised Signal*: In addition to label noisy learning, we incorporate self-supervised learning techniques into the training process. By designing these auxiliary tasks carefully, we can encourage the model to learn more robust and invariant representations, which can help mitigate the effects of label noise and improve generalization performance. Specifically, our second method to obtain positive feature involves performing semantically invariant image augmentation on the anchor point x :

$$f(x_s^+) = f(\mathcal{T}(x)), \quad (9)$$

where $\mathcal{T}(\cdot)$ is a stochastic data augmentation module that applies random transformations to a given data example x , generating two correlated views referred to as x_{s1}^+ and x_{s2}^+ , which we consider as a positive pair. Follow SimCLR [22], we employ a sequential application of three simple augmentations: random cropping and flipping followed by resizing back to the original size, random color distortions, and random Gaussian blur.

Our third method to obtain positive examples involving a mixture of positive feature representations, which can be seen as a mixup of positive samples to obtain the most representative positive instances:

$$f(x_m^+) = \frac{1}{M} \sum_{i=1}^M f(x_i). \quad (10)$$

The positive feature representation $f(x_m^+)$ obtained from the equation above represents the class centroid of M positive examples $\{x_i\}_{i=1}^M$. In other words, it synthesizes a virtual representative positive sample, which is also referred to as feature augmentation. This method helps overcome the challenge of instance-level contrast, where each instance is treated as a separate class. By synthesizing a virtual sample that represents the class centroid, the feature representation of each instance is

TABLE I
AU OCCURRENCE RATES (%) IN THE TRAINING SETS OF DIFFERENT DATASETS. "-" DENOTES THE AU IS NOT ANNOTATED IN THIS DATASET.

Dataset	AU Index														
	1	2	4	6	7	9	10	12	14	15	17	23	24	25	26
BP4D [63]	21.1	17.1	20.3	46.2	54.9	-	59.4	56.2	46.6	16.9	34.4	16.5	15.2	-	-
DISFA [64]	5.0	4.0	15.0	8.1	-	4.3	-	13.2	-	-	-	-	-	27.8	8.9
GFT [65]	3.7	13.5	3.7	28.3	-	-	24.6	29.3	3.1	10.7	-	25.0	14.1	-	-
Aff-Wild2 [66]	11.9	5.1	16.0	26.5	39.9	-	34.5	24.3	-	2.8	-	3.1	2.8	62.8	7.6

encouraged to be closer to the class centroid, which is benefit of capturing the essential characteristics of the positive class.

The aforementioned three methods of obtaining positive examples combine the use of label noisy learning for supervised signals and data augmentation for self-supervised signals. These three types of positive examples are randomly mixed with probabilities p_1 , p_2 , and p_3 respectively, where $p_1 + p_2 + p_3 = 1$. Our approach aims to improve the quality of supervised signals utilized in the training process. By integrating these techniques, we effectively mitigate the impact of noisy and false labels, increase the resilience of models to errors and variations in labeled datasets, and ultimately enhance the generalization ability of models to unseen data.

By addressing the above three challenges, our approach improves the encoding capability of the shared encode, ultimately leading to improved generalization performance in AU detection. The pseudocode for the algorithm is provided in Algorithm. 1.

Algorithm 1 The proposed AUNCE algorithm

Input: Mini batch data \mathcal{R} , feature representation function $f(\cdot)$, p_1 , p_2 , and p_3 , β .

Output: Parameters Θ .

for sample $x \in \mathcal{R}$ **do**

 Obtain positive sample set $\{x_i^+\}_{i=1}^M \in \mathcal{R}$;

 Obtain negative sample set $\{x_j^-\}_{j=1}^N \in \mathcal{R}$;

$p = \text{random.uniform}(0,1)$;

if $p \leq p_1$ **then**

 Obtain $f(x_h^+)$ via Eq (8)

if $p_1 < p \leq p_1 + p_2$ **then**

 Obtain $f(x_s^+)$ via Eq (9)

else

 Obtain $f(x_m^+)$ via Eq (10)

 Calculate AUNCE loss via Eq (4);

 Update Θ .

Result: Parameters Θ .

IV. EVALUATION

A. Experiment Setting

1) *Datasets*: In our experiments, we extensively utilize three well-established datasets in constrained scenarios for AU detection, namely BP4D [63], DISFA [64], GFT [65], and one well-established dataset in unconstrained scenarios, namely Aff-Wild2 [66]. Our primary focus is on assessing frame-level AU detection, as opposed to datasets that solely provide video-level annotations.

BP4D [63]: This dataset comprises 41 participants, including 23 females and 18 males. Each individual is featured in 8 sessions, recorded using both 2D and 3D videos. The dataset encompasses approximately 140,000 frames, each annotated with AU labels indicating occurrence or non-occurrence. Additionally, each frame is meticulously annotated with 68 facial landmarks detected using the SDM [67] method. For BP4D dataset, we employ a three-fold cross-validation methodology for rigorous evaluation.

DISFA [64]: This dataset is composed of 27 videos, recorded from 15 men and 12 women. Each video comprises 4,845 frames, resulting in a total of 130,788 images. Frames in this dataset are annotated with AU intensities ranging from 0 to 5, and 68 facial landmarks are detected using the AAM [68] method. Frames with intensities equal to or greater than 2 are considered positive, while others are classified as negative. We also employ the same three-fold cross-validation methodology as BP4D dataset for rigorous evaluation of DISFA dataset.

GFT [65]: This dataset comprises 96 participants, organized into 32 groups of three individuals, engaged in unscripted conversations. Each participant is recorded via video, with the majority of frames capturing moderate out-of-plane poses. Annotations for each frame include 10 AUs, alongside 68 facial landmarks identified using the ZFace [69] tool. In accordance with the standard training and testing partitions, our training set consists of 78 participants, amounting to approximately 108,000 frames, while the testing set includes 18 participants, totaling around 24,600 frames.

Aff-Wild2 [66]: This dataset is an extensive in-the-wild facial expression dataset, with videos sourced from YouTube, encompassing a broad range of ages, ethnicities, professions, emotions, poses, lighting conditions, and occlusions. This dataset comprises 305 videos, totaling approximately 1,390,000 frames for the training set, and 105 videos, with around 440,000 frames for the validation set. Each frame is annotated with 12 AUs. For facial landmark annotations, we utilize the Dlib library [70], [71] for detecting 68 facial landmarks per frame. Following the methodology of Zhang et al. [72], we train our AUNCE on the training set and evaluate it on the validation set.

The occurrence rates of AUs in the training sets of these datasets are presented in Table I. It is evident from the table that the class imbalance issue of each type of AU is prevalent across all datasets, especially on the DISFA, GFT and Aff-Wild2 datasets.

2) *Implementation Details*: Initially, the 68 facial landmarks undergo a conversion into 49 facial internal landmarks,

TABLE II
QUANTITATIVE COMPARISON RESULTS ON BP4D DATASET, WHERE THE EVALUATION METRIC IS F1-SCORE(%).

Method	Source	AU Index												Avg.
		1	2	4	6	7	10	12	14	15	17	23	24	
EAC-Net [7]	2018 TPAMI	39.0	35.2	48.6	76.1	72.9	81.9	86.2	58.8	37.5	59.1	35.9	35.8	55.9
ROI [4]	2017 CVPR	36.2	31.6	43.4	77.1	73.7	85.0	87.0	62.6	45.7	58.0	38.3	37.4	56.4
ARL [15]	2019 TAC	45.8	39.8	55.1	75.7	77.2	82.3	86.6	58.8	47.6	62.1	47.4	55.4	61.1
MAL [75]	2023 TAC	47.9	49.5	52.1	77.6	77.8	82.8	88.3	66.4	49.7	59.7	45.2	48.5	62.2
JAA-Net [14]	2021 IJCV	53.8	47.8	58.2	78.5	75.8	82.7	88.2	63.7	43.3	61.8	45.6	49.9	62.4
GLEE-Net [20]	2024 TCSVT	60.6	44.4	61.0	80.6	78.7	85.4	88.1	64.9	53.7	65.1	47.7	58.5	65.7
MMA-Net [76]	2023 PRL	52.5	50.9	58.3	76.3	75.7	83.8	87.9	63.8	48.7	61.7	46.5	54.4	63.4
SEV-Net [77]	2021 CVPR	58.2	50.4	58.3	81.9	73.9	87.7	87.5	61.6	52.6	62.2	44.6	47.6	63.9
HMP-PS [78]	2021 CVPR	53.1	46.1	56.0	76.5	76.9	82.1	86.4	64.8	51.5	63.0	49.9	54.5	63.4
AAR [79]	2023 TIP	53.2	47.7	56.7	75.9	79.1	82.9	88.6	60.5	51.5	61.9	51.0	56.8	63.8
ISTR [80]	2021 ACM MM	54.0	46.0	55.7	79.4	78.8	84.5	87.0	67.0	55.6	63.1	50.7	55.3	64.8
MEGraph [56]	2022 IJCAI	52.7	44.3	60.9	79.9	80.1	85.3	89.2	69.4	55.4	64.4	49.8	55.1	65.5
SimCLR [22]	2020 ICML	38.0	36.4	37.2	66.6	64.7	76.2	76.2	51.1	29.8	56.1	27.5	37.7	49.8
MoCo [32]	2020 CVPR	30.8	41.3	42.1	70.2	70.4	78.7	82.5	53.3	25.2	59.1	31.5	34.3	51.6
CLP [28]	2023 TIP	47.7	50.9	49.5	75.8	78.7	80.2	84.1	67.1	52.0	62.7	45.7	54.8	62.4
BTFM [81]	2023 CVPR	57.4	52.6	64.6	79.3	81.5	82.7	85.6	67.9	47.3	58.0	47.0	44.9	64.1
SupHCL [49]	2022 ACM MM	52.8	45.7	61.6	79.5	79.3	84.7	86.9	67.6	51.4	62.5	48.6	52.3	64.4
KSRL [46]	2022 CVPR	53.3	47.4	56.2	79.4	80.7	85.1	89.0	67.4	55.9	61.9	48.5	49.0	64.5
CLEF [82]	2023 ICCV	55.8	46.8	63.3	79.5	77.6	83.6	87.8	67.3	55.2	63.5	53.0	57.8	65.9
AUNCE(Ours)	-	53.6	49.8	61.6	78.4	78.8	84.7	89.6	67.4	55.1	65.4	50.9	58.0	66.1
		(±0.15)	(±0.12)	(±0.17)	(±0.21)	(±0.19)	(±0.22)	(±0.22)	(±0.17)	(±0.14)	(±0.15)	(±0.14)	(±0.15)	(±0.17)

excluding those associated with the facial contour. Subsequently, the images undergo augmentation through similarity transformation, encompassing in-plane rotation, uniform scaling, and translation, utilizing the 49 facial landmarks. The resulting images are standardized to a resolution of $256 \times 256 \times 3$ pixels and then randomly cropped into $224 \times 224 \times 3$ pixels, with the addition of a random horizontal flip.

For the training process, the encoder is conducted on one NVIDIA GeForce RTX 3090 GPU with 24GB for one day and implemented by PyTorch using an AdamW optimizer with $\beta_1=0.9$, $\beta_2=0.999$ and weight decay of 10^{-6} . We set a learning rate of 10^{-5} and 60 epochs. Due to our discriminative contrastive learning framework that sample pairs are selected in a same batch, so the batch size has a strong influence on the experimental results. In terms of the hyperparameters in AUNCE, n_{au} is set as 12 for BP4D and 8 for DISFA respectively, the number K for choosing nearest neighbors in the ANFL [56] is set to 4, and the temperature coefficient τ is 0.5. The analysis for β and p_1, p_2, p_3 will introduce in Section. IV-D2.

In assessing the acquired representations, we adhere to the established linear evaluation protocol, as commonly employed in previous studies [22], [27], [73], [74]. This involves training a linear classifier atop the fixed base network, and the highest test accuracy across our models serves as a surrogate measure for the quality of the learned representations.

3) *Evaluation Metrics*: Aligned with current state-of-the-art methodologies, we utilized two prevalent frame-based metrics for AU detection: F1-score(%) and Accuracy(%). F1-score represents the harmonic mean of precision and recall, widely employed in the context of AU detection. For each approach, we calculate average metrics across all AUs (denoted as Avg.).

B. Comparison with State-of-the-Art Methods

1) *Evaluation on BP4D*: Since we use AU labels to assist the process of selecting positive sample pairs, we introduce five groups of supervised AU detection frameworks to compare with our method. The quantitative results of state-of-the-art methods from the past seven years for BP4D dataset are shown in Table II. AUNCE exhibits superior performance in AU detection when contrasted with alternative approaches.

Methods in the first group are based on feature extraction of regional area around AUs, including EAC-Net [7], ROI [4] and ARL [15]. Our approach achieves a notable improvement, with an increase in F1-score ranging from 5.0% to 10.2% over these methods. This advancement is primarily due to early feature extraction methods neglecting critical correlation information among AUs and failing to specifically address the class imbalance issue for each AU. Furthermore, the precision of the encoders utilized by these methods is generally lower.

Methods in the second group are based on a multi-task learning strategy, including JAA-Net [14], MAL [75] and GLEE-Net [20]. Our method surpasses MAL by 3.9%, primarily due to the ability of AUNCE to help the encoder address the class imbalance issue among different AUs, and the facial expression recognition component in MAL introduces some negative transfer effects on AU detection. The 3.7% improvement over JAA-Net can be attributed to the influence of the facial landmark detection task within the multi-task learning framework on AU detection, which is also affected by the weighting of different losses. Additionally, the modest 0.4% improvement over GLEE-Net is due to the relatively limited impact of 3D facial reconstruction task on enhancing the performance of 2D AU detection.

Methods in the third group mainly utilize the AU semantic prior knowledge, including MMA-Net [76] and SEV-Net [77]. Our approach demonstrates an average improvement of 2.7%

TABLE III
QUANTITATIVE COMPARISON RESULTS ON DISFA DATASET, WHERE THE EVALUATION METRIC IS F1-SCORE(%).

Method	Source	AU Index								Avg.
		1	2	4	6	9	12	25	26	
EAC-Net [7]	2018 TPAMI	41.5	26.4	66.4	50.7	80.5	89.3	88.9	15.6	48.5
ROI [4]	2017 CVPR	41.5	26.4	66.4	50.7	80.5	89.3	88.9	15.6	48.5
ARL [15]	2019 TAC	43.9	42.1	63.6	41.8	40.0	76.2	95.2	66.8	58.7
MAL [75]	2023 TAC	43.8	39.3	68.9	47.4	48.6	72.7	90.6	52.6	58.0
JAA-Net [14]	2021 IJCV	62.4	60.7	67.1	41.1	45.1	73.5	90.9	67.4	63.5
GLEE-Net [20]	2024 TCSVT	61.9	54.0	75.8	45.9	55.7	77.6	92.9	60.0	65.5
SEV-Net [77]	2021 CVPR	55.3	53.1	61.5	53.6	38.2	71.6	95.7	41.5	58.8
MMA-Net [76]	2023 PRL	63.8	54.8	73.6	39.2	61.5	73.1	92.3	70.5	66.0
HMP-PS [78]	2021 CVPR	38.0	45.9	65.2	50.9	50.8	76.0	93.3	67.6	61.0
ISTR [80]	2021 ACM MM	47.5	53.3	64.4	51.8	44.4	74.7	92.1	60.7	61.1
MEGraph [56]	2022 IJCAI	52.5	45.7	76.1	51.8	46.5	76.1	92.9	57.6	62.4
AAR [79]	2023 TIP	62.4	53.6	71.5	39.0	48.8	76.1	91.3	70.6	64.2
SIMCLR [22]	2020 ICML	21.2	23.3	47.5	42.4	35.5	66.8	81.5	52.7	46.4
MoCo [32]	2020 CVPR	22.7	18.2	45.9	45.4	34.1	72.9	83.4	54.5	47.1
CLP [28]	2023 TIP	42.4	38.7	63.5	59.7	38.9	73.0	85.0	58.1	57.4
BTFM [81]	2023 CVPR	41.5	44.9	60.3	51.5	50.3	70.4	91.3	55.3	58.2
SupHCL [49]	2022 ACM MM	52.5	58.8	70.0	53.5	51.4	73.1	95.6	58.0	64.1
KSRL [46]	2022 CVPR	60.4	59.2	67.5	52.7	51.5	76.1	91.3	57.7	64.5
CLEF [82]	2023 ICCV	64.3	61.8	68.4	49.0	55.2	72.9	89.9	57.0	64.8
AUNCE(Ours)	-	61.8	58.9	74.9	49.7	56.2	73.5	92.1	64.2	66.4
		(±0.37)	(±0.22)	(±0.42)	(±0.31)	(±0.36)	(±0.49)	(±0.42)	(±0.28)	(±0.36)

TABLE IV
QUANTITATIVE COMPARISON RESULTS ON GFT DATASET, WHERE THE EVALUATION METRIC IS F1-SCORE(%).

Method	Source	AU Index										Avg.
		1	2	4	6	10	12	14	15	23	24	
AlexNet [83]	2012 NIPS	44	46	2	73	72	82	5	19	43	42	42.8
LSVM [84]	2008 JMLR	38	32	13	67	64	78	15	29	49	44	42.9
TCAE [85]	2019 CVPR	43.9	49.5	6.3	71.0	76.2	79.5	10.7	28.5	34.5	41.7	44.2
CPAM [86]	2020 TBIOM	43.7	44.9	19.8	74.6	76.5	79.8	50.0	33.9	16.8	12.9	45.3
TAE [87]	2022 TPAMI	46.3	48.8	13.4	76.7	74.8	81.8	19.9	42.3	50.6	50.0	50.5
EAC-Net [7]	2018 TPAMI	15.5	56.6	0.1	81.0	76.1	84.0	0.1	38.5	57.8	51.2	46.1
ARL [15]	2019 TAC	51.9	45.9	13.7	79.2	75.5	82.8	0.1	44.9	59.2	47.5	50.1
JAA-Net [14]	2021 IJCV	46.5	49.3	19.2	79.0	75.0	84.8	44.1	33.5	54.9	50.7	53.7
AAR [79]	2023 TIP	66.3	53.9	23.7	81.5	73.6	84.2	43.8	53.8	58.2	46.5	58.5
MAL [75]	2023 TAC	52.4	57.0	54.1	74.5	78.0	84.9	43.1	47.7	54.4	51.9	59.8
MoCo [32]	2020 CVPR	35.9	45.4	13.5	83.4	71.3	78.1	23.3	37.3	26.6	50.7	46.5
SimCLR [22]	2020 ICML	39.6	48.3	5.6	80.7	76.2	80.6	18.1	41.6	46.1	43.8	48.1
CLP [28]	2023 TIP	44.6	58.7	34.7	75.9	78.6	86.6	20.3	44.8	56.4	42.2	54.3
AUNCE(Ours)	-	53.6	62.8	51.3	80.6	82.1	88.2	48.2	49.8	54.6	58.9	63.0
		(±0.33)	(±0.18)	(±0.28)	(±0.24)	(±0.41)	(±0.11)	(±0.35)	(±0.23)	(±0.42)	(±0.35)	(±0.29)

TABLE V
QUANTITATIVE COMPARISON RESULTS ON AFF-WILD2 DATASET, WHERE THE EVALUATION METRIC IS F1-SCORE(%).

Method	Source	AU Index										Avg.		
		1	2	4	6	7	10	12	15	23	24		25	26
EAC-Net [7]	2018 TPAMI	49.6	33.7	55.6	66.4	82.3	81.4	76.9	11.8	12.5	12.2	93.7	26.8	50.2
ARL [15]	2019 TAC	59.2	48.2	54.9	70.0	83.4	80.3	72.0	0.1	0.1	17.3	93.0	37.5	51.3
JAA-Net [14]	2021 IJCV	61.7	50.1	56.0	71.7	81.7	82.3	78.0	31.1	1.4	8.6	94.8	37.5	54.6
PASN [72]	2021 ICCV	65.7	64.2	66.5	76.6	74.7	72.7	78.6	18.5	10.6	55.1	80.7	41.7	58.8
AAR [79]	2023 TIP	65.4	57.9	59.9	73.2	84.6	83.2	79.9	21.8	27.4	19.9	94.5	41.7	59.1
AUNCE(Ours)	-	68.8	67.6	64.7	74.8	88.6	78.4	81.3	26.9	36.7	18.6	96.1	43.8	62.2
		(±0.25)	(±0.37)	(±0.28)	(±0.33)	(±0.12)	(±0.47)	(±0.31)	(±0.17)	(±0.08)	(±0.42)	(±0.39)	(±0.32)	(±0.29)

and 2.2%, respectively. This phenomenon can be attributed to the inherent limitations of these methods in effectively capturing and representing the distinct information encoded within Action Units (AUs) using simple semantic descriptions.

Methods in the fourth group focus on capturing correlational information among AUs, including HMP-PS [78], AAR [79], ISTR [80] and MEGraph [56]. Our approach exhibits a performance advantage of approximately 0.6%-2.7% in F1-

score. This underscores the efficacy of our supervised discriminative contrastive learning paradigm in effectively capturing differential information instead of pixel-level information. It is noteworthy that the encoder used in our method is only the same as the network MEGraph used for the first stage of training, with reduced parameters by nearly 7M. This highlights the applicability of AUNCE to more lightweight network structures and emphasizes that learning only the difference information among features is more potent than learning the pixel-level information of the entire image.

Methods in the last group are based on contrastive learning, including SIMCLR [22], MoCo [32], CLP [28], BTFM [81], SupHCL [49], KSRL [46] and CLEF [82]. When compared to these methods, our approach demonstrates a performance advantage of approximately 0.2% to 16.3% in F1-score. This improvement is attributed to the efficacy of our proposed negative sample re-weighting strategy and positive sample sampling strategy, specifically tailored for the AU detection task using static images.

2) *Evaluation on DISFA*: Comparable outcomes are evident in the DISFA dataset, as outlined in Table III, where AUNCE attains the highest overall performance in AU detection. Furthermore, a comparison between Table II and Table III reveals that recent methods such as SEV-Net, MEGraph, and BTFM demonstrate strong performance on the BP4D dataset but achieve only mediocre results on the DISFA dataset. This disparity suggests their limited generalizability. The more pronounced class imbalance issue in DISFA, as shown in Table I, likely contributes to this performance gap. In contrast, AUNCE consistently delivers robust performance on both BP4D and DISFA datasets and achieves more stable results across various AUs due to our proposed negative sample re-weighting strategy.

3) *Evaluation on GFT*: Table IV presents the F1-score results on the GFT dataset, where our AUNCE method demonstrates significantly superior performance compared to previous approaches. Unlike BP4D and DISFA, which primarily consist of near-frontal face images, GFT includes many images captured under out-of-plane poses. In this challenging scenario, other methods such as EAC-Net, ARL and CLP so on struggle to perform well. In contrast, AUNCE achieves a commendable average F1-score of 63.0%.

4) *Evaluation on Aff-Wild2*: We have validated the performance of our AUNCE method in constrained scenarios. To further assess its effectiveness in unconstrained scenarios, we compared it with other approaches on the challenging Aff-Wild2 dataset, as shown in Table V. Our AUNCE method demonstrates a higher average F1-score than previous methods. Notably, while EAC-Net and PASN leverage external training data, our method achieves superior overall performance using only the Aff-Wild2 dataset. By comparing the results of ARL, JAA-Net, AAR to our AUNCE method across Table II to Table V, it is evident that the performance margins between our AUNCE method and other methods on GFT and Aff-Wild2 are larger than those on BP4D and DISFA. This indicates that AUNCE is more effective at handling challenging cases in AU detection.

C. Ablation Study

TABLE VI
COMPARISON OF THE WEIGHTED CROSS-ENTROPY (WCE) LOSS AND AUNCE WITH DIFFERENT ENCODERS ON BP4D DATASET.

Backbone	Source	Loss	F1-Score(%)	Accuracy(%)
ResNet18 [88]	2016CVPR	WCE	52.3	73.8
		AUNCE	54.9 ^{2.6↑}	74.3 ^{0.5↑}
ResNet50 [88]	2016CVPR	WCE	56.2	75.5
		AUNCE	59.7 ^{3.5↑}	77.0 ^{1.5↑}
ROI [4]	2017CVPR	WCE	56.4	75.9
		AUNCE	58.8 ^{2.4↑}	76.7 ^{0.8↑}
ARL [15]	2019TAC	WCE	61.1	78.2
		AUNCE	62.9 ^{1.8↑}	79.1 ^{0.9↑}
JAA-Net [14]	2021IJCV	WCE	62.4	78.6
		AUNCE	64.1 ^{1.7↑}	80.2 ^{1.6↑}
MEGraph [56] (Onestage)	2022IJCAI	WCE	63.6	80.0
		AUNCE	66.1 ^{2.5↑}	80.4 ^{0.4↑}

1) *Compared with weighted cross-entropy loss*: Due to the primary innovation of this paper being the introduction of a novel contrastive loss, AUNCE, which is compatible with various AU detection encoders, we conducted a comparative analysis between the proposed AUNCE loss and the traditional weighted cross-entropy loss (WCE) across multiple AU detection encoders, as detailed in Table VI. The findings reveal that AUNCE demonstrates superior performance in AU detection. Notably, the MEGraph encoder achieved the best results, with the F1-score on the BP4D dataset improving from 63.6% to 66.1%. This underscores the effectiveness of capturing unique features of different samples over focusing solely on pixel-level information. Furthermore, we optimized the two-stage training process of MEGraph into a single-stage process, significantly reducing both the training time and the number of parameters required for the model.

2) *Evaluating other components*: We further evaluate the effectiveness of weight coefficient w_i , negative sample re-weighting strategy and positive sample sampling strategy. Quantitative results of our method with the above component combinations are summarized in Table VII. The baseline (BL) is rooted in SIMCLR [22], but positive sample pairs are changed to images with the highest similarity to original images. Other components are the weight coefficient for both WCE and AUNCE (w_i), the positive sample sampling strategy (PS), and the negative sample re-weighting strategy (NS).

Weight coefficient w_i : The weights w_i have been pointed out as a fixed value in Section. III-A, which achieve an increase of 0.9% in F1-score and 0.2% in Accuracy. For an AU, its activation indicator is a binary variable, and the corresponding information content can be measured using entropy: $-\log(p_i)$. Therefore, AUs with lower activation probabilities carry more information and should be assigned higher weights. This forms the theoretical basis for our weighting strategy.

Positive sample sampling strategy: As outlined in Table VII, the positive sample sampling strategy contributes to a 2.8% increase in F1-score and a 0.5% improvement in Accuracy compared to model B. This validates that selecting different types of positive sample pairs with appropriate prob-

TABLE VII
QUANTITATIVE RESULTS OF ABLATION STUDY ON BP4D DATASET.

Model	BL	wi	PS	NS	AU Index										F1-Score(%)	Accuracy(%)		
					1	2	4	6	7	10	12	14	15	17			23	24
A	✓				39.8	44.3	58.8	76.0	77.7	76.9	88.0	64.5	49.0	59.0	43.5	43.4	60.1	79.1
B	✓	✓			40.1	43.0	58.9	75.4	79.3	78.8	87.8	64.1	48.7	61.0	46.9	47.5	61.0 ^{0.9↑}	79.3 ^{0.2↑}
C	✓	✓	✓		51.1	45.6	58.3	77.5	77.0	84.5	89.0	63.7	54.6	65.5	46.8	53.3	63.8 ^{3.7↑}	79.8 ^{0.7↑}
D	✓	✓		✓	50.2	43.0	58.7	77.9	77.3	83.7	88.7	64.2	53.9	64.9	50.0	56.4	64.1 ^{4.0↑}	79.9 ^{0.8↑}
E	✓	✓	✓	✓	53.6	49.8	61.6	78.4	78.8	84.7	89.6	67.4	55.1	65.4	50.9	58.0	66.1 ^{6.0↑}	80.4 ^{1.3↑}

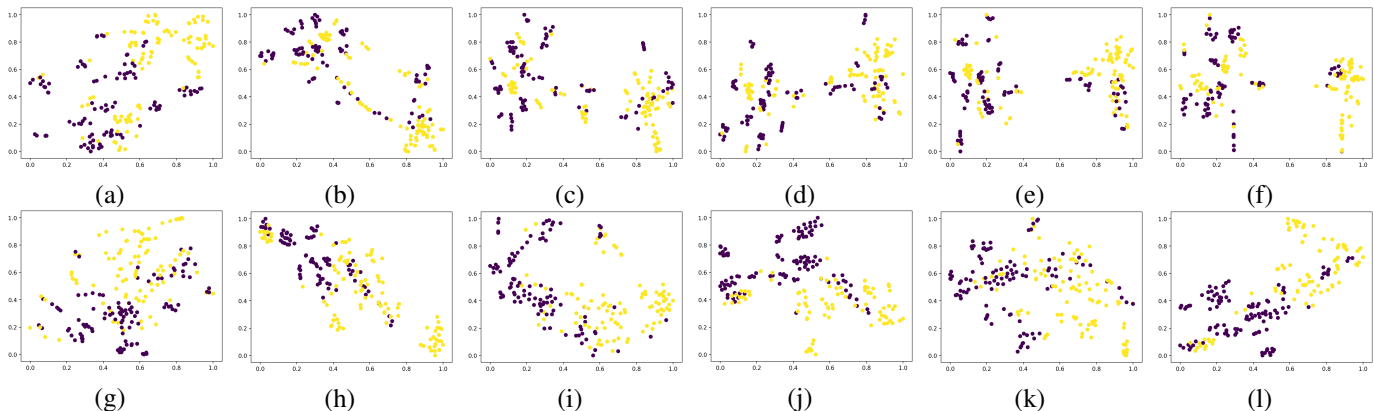


Fig. 4. T-SNE visualization of feature representations on BP4D and DISFA datasets. Colors indicates whether AU1 exists. Top row: (a) Representations optimized by WCE on BP4D dataset, and (b)-(f) Visualizations of ablation study on BP4D dataset, respectively represent model A-E. Bottom row: (g) Representations optimized by AUNCE on DISFA dataset, and (h)-(l) Visualizations of ablation study on DISFA dataset, respectively represent model A-E.

abilities can mitigate issues arising from AU labels tainted by noise and errors. The strategy achieves this by incorporating three types of positive sample pairs: the self-supervised signal pair, the highest similarity pair, and the mixed positive features pair. These pairs provide the models with diverse information from various views, thereby enhancing the generalization ability of the contrastive learning framework.

Negative sample re-weighting strategy: The negative sample re-weighting strategy to minority AUs results in a 3.1% increase in F1-score and a 0.6% increase in Accuracy compared to model B. This illustrates that the strategy can change the backpropagation gradient of minority and majority class samples, facilitating faster label category gradient updates with a smaller number of samples. Additionally, model E achieves an average increase of 2.3% in F1-score compared to model C, further supporting the efficacy of the re-weighting strategy.

We further show the visualization using T-SNE dimensionality reduction of the learned feature representations optimized by AUNCE and WCE to qualitatively assess the efficacy of our proposed discriminative contrastive learning paradigm, as illustrated in Fig. 4. For each dataset, a random sample of 200 images is utilized for illustration purposes. A comparison between Fig. 4(a), Fig. 4(f) against Fig. 4(g), Fig. 4(l) reveals that the learned representations optimized by AUNCE exhibit greater separability than those optimized by WCE. Additionally, Fig. 4(b)-(f) and Fig. 4(g)-(l) qualitatively showcase the effectiveness of each component in our ablation study.

Based on all ablation studies, it demonstrates that our proposed discriminative contrastive learning paradigm enhances

the encoding capability of the shared encoder, improves classification accuracy by addressing the class imbalance issue of each AU type, and bolsters model robustness against AU labels affected by noise and errors. This, in turn, leads to enhanced generalization performance in AU detection. The introduction of each component proves beneficial for performance improvement, with NS emerging as the most effective component. Moreover, the results on each AU are also shown in Table VII. It can be seen that the results on basically every AU have improved or approached after we add w_i , PS and NS.

D. Hyperparameters Analysis

TABLE VIII
QUANTITATIVE RESULTS THE PROBABILITIES OF VARIOUS POSITIVE SAMPLE PAIRS p_1, p_2, p_3, p_4 ON BP4D DATASET.

	p_1	p_2	p_3	p_4	F1-Score(%)
Probabilities	1	0	0	0	60.1
	0	1	0	0	48.4
	0	0	1	0	63.2
	0	0	0	1	17.6
	0.1	0.1	0.8	0	63.8
	0.15	0.15	0.7	0	66.1
	0.2	0.2	0.6	0	65.7
	0.25	0.25	0.5	0	65.2
	0.3	0.3	0.4	0	64.3
	0.4	0.4	0.2	0	58.8

1) p_1, p_2, p_3, p_4 , the probabilities of various positive sample pairs: In our paper, p_1 represents the probabilities of images

with the highest similarity to original images, p_2 represents the probabilities of self-supervised images enhanced by simple augmentations, p_3 represents the probabilities of a mixture of all positive samples, and p_4 represents the probabilities of images with the lowest similarity to original images. Given that p_1 , p_2 , p_3 , and p_4 address the problem of AU labels tainted by noise and errors, we systematically vary these probabilities from 0 to 1 to investigate their impact on our framework. As p_1 and p_2 are deemed reliable positive samples, we set their values to be the same during the variation.

The experimental results are presented in Table VIII. When $p_1=0.15$, $p_2=0.15$, $p_3=0.7$, and $p_4=0$, the experimental result is optimal. It is observed that images with the lowest similarity to original images contribute minimally to the training process, as these images essentially represent noise and errors. The conclusion is consistent with [89], [90]. The mixture of all positive samples plays a pivotal role, as it encourages the feature representation of each instance to be closer to the class centroid, facilitating the capture of essential characteristics of the positive class. The indispensability of the remaining two positive samples lies in their ability to mitigate the impact of noisy and false samples, thereby reinforcing the robustness of the training process.

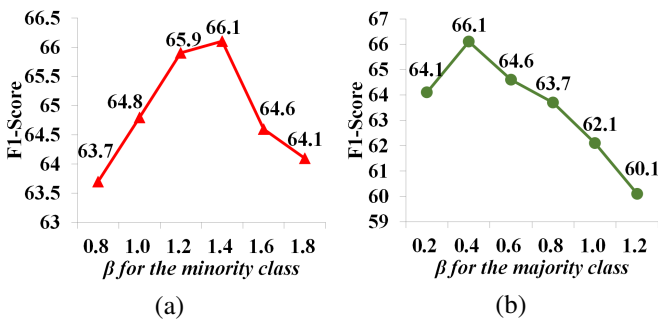


Fig. 5. Quantitative results of β of different positive and negative samples for each AU type on BP4D dataset. From left to right: (a) β for positive samples (the minority class), and (b) β for negative samples (the majority class).

2) *Backpropagation rate controller β* : As is well understood, the hyperparameter β plays a crucial role in governing the relative importance of minority and majority class samples during the parameter update process. It ensures that the model allocates more attention to minority class samples when necessary and balances the gradient magnitudes accordingly. To explore its effects, we systematically vary the hyperparameter β for the minority class from 0.8 to 1.8, with β for the majority class fixed at 0.4. Additionally, we vary β for the majority class from 0.2 to 1.2, keeping β for the minority class fixed at 1.2.

The experimental results are depicted in Fig. 5. The optimal experimental outcome is observed when β for the minority class is set to 1.2, and β for the majority class is fixed at 0.4. Hence, when $\beta_{\text{minority}} > \beta_{\text{majority}}$, the impact of the class imbalance issue can be effectively mitigated.

V. CONCLUSION

In this paper, we introduce a contrastive learning framework for AU detection. Our proposed contrastive loss, named AUNCE, shares similarities with InfoNCE, transforming the

task of learning entire pixel-level information of AUs into the more effective learning of subtle feature differences when AUs activate. Additionally, we present a positive sample sampling strategy that introduces three types of positive sample pairs, addressing the challenge of AU labels tainted by noise and errors in two AU datasets. To further enhance the framework, we incorporate a negative sample re-weighting strategy specifically aimed for minority AUs. This strategy controls the relative contribution of minority class samples to the parameter updates, effectively addressing the class imbalance issue of each AU type, and contributing to hard negative sample mining. Experimental results underscore the superior performance of AUNCE in comparison to existing methods.

ACKNOWLEDGEMENT

This research was supported by the National Natural Science Foundation of China (Nos. 62176221, 61572407), and Sichuan Science and Technology Program (Nos. 2024NS-FTD0036, 2024ZHCG0166). The computation is completed in the HPC Platform of Huazhong University of Science and Technology.

REFERENCES

- [1] E. L. Rosenberg and P. Ekman, *What the face reveals: Basic and applied studies of spontaneous expression using the Facial Action Coding System (FACS)*. Oxford University Press, 2020.
- [2] M. Dahmane and J. Meunier, "Prototype-based modeling for facial expression analysis," *IEEE Transactions on Multimedia*, vol. 16, no. 6, pp. 1574–1584, 2014.
- [3] K. Zhao, W.-S. Chu, and H. Zhang, "Deep region and multi-label learning for facial action unit detection," in *Proc. CVPR*, 2016, pp. 3391–3399.
- [4] W. Li, F. Abtahi, and Z. Zhu, "Action unit detection with region adaptation, multi-labeling learning and optimal temporal fusing," in *Proc. CVPR*, 2017, pp. 1841–1850.
- [5] X. Xiang and T. D. Tran, "Linear disentangled representation learning for facial actions," *IEEE Transactions on Circuits and Systems for Video Technology*, vol. 28, no. 12, pp. 3539–3544, 2017.
- [6] C. Corneanu, M. Madadi, and S. Escalera, "Deep structure inference network for facial action unit recognition," in *Proc. ECCV*, 2018, pp. 298–313.
- [7] W. Li, F. Abtahi, Z. Zhu, and L. Yin, "Eac-net: Deep nets with enhancing and cropping for facial action unit detection," *IEEE transactions on pattern analysis and machine intelligence*, vol. 40, no. 11, pp. 2583–2596, 2018.
- [8] C. Ma, L. Chen, and J. Yong, "Au r-cnn: Encoding expert prior knowledge into r-cnn for action unit detection," *Neurocomputing*, vol. 355, pp. 35–47, 2019.
- [9] B. Taha, M. Hayat, S. Berretti, D. Hatzinakos, and N. Werghi, "Learned 3d shape representations using fused geometrically augmented images: Application to facial expression and action unit detection," *IEEE Transactions on Circuits and Systems for Video Technology*, vol. 30, no. 9, pp. 2900–2916, 2020.
- [10] A. Bauer, D. Wollherr, and M. Buss, "Human-robot collaboration: a survey," *International Journal of Humanoid Robotics*, vol. 5, no. 01, pp. 47–66, 2008.
- [11] D. McDuff, R. El Kaliouby, D. Demirdjian, and R. Picard, "Predicting online media effectiveness based on smile responses gathered over the internet," in *2013 10th IEEE international conference and workshops on automatic face and gesture recognition (FG)*. IEEE, 2013, pp. 1–7.
- [12] G. Szirtes, D. Szolgay, Á. Utasi, D. Takács, I. Petrás, and G. Fodor, "Facing reality: An industrial view on large scale use of facial expression analysis," in *Proc. EmotiW*, 2013, pp. 1–8.
- [13] F. Vicente, Z. Huang, X. Xiong, F. De la Torre, W. Zhang, and D. Levi, "Driver gaze tracking and eyes off the road detection system," *IEEE Transactions on Intelligent Transportation Systems*, vol. 16, no. 4, pp. 2014–2027, 2015.

- [14] Z. Shao, Z. Liu, J. Cai, and L. Ma, "Jaa-net: Joint facial action unit detection and face alignment via adaptive attention," *International Journal of Computer Vision*, vol. 129, no. 2, pp. 321–340, 2021.
- [15] Z. Shao, Z. Liu, J. Cai, Y. Wu, and L. Ma, "Facial action unit detection using attention and relation learning," *IEEE transactions on affective computing*, 2019.
- [16] G. Li, X. Zhu, Y. Zeng, Q. Wang, and L. Lin, "Semantic relationships guided representation learning for facial action unit recognition," in *Proc. AAAI*, vol. 33, no. 01, 2019, pp. 8594–8601.
- [17] T. Song, L. Chen, W. Zheng, and Q. Ji, "Uncertain graph neural networks for facial action unit detection," in *Proc. AAAI*, vol. 35, no. 7, 2021, pp. 5993–6001.
- [18] S. Wang, Y. Chang, and C. Wang, "Dual learning for joint facial landmark detection and action unit recognition," *IEEE Transactions on Affective Computing*, 2021.
- [19] J. Yang, Y. Hristov, J. Shen, Y. Lin, and M. Pantic, "Toward robust facial action units' detection," *Proc. IEEE*, 2023.
- [20] W. Zhang, L. Li, Y. Ding, W. Chen, Z. Deng, and X. Yu, "Detecting facial action units from global-local fine-grained expressions," *IEEE Transactions on Circuits and Systems for Video Technology*, 2024.
- [21] Z. Wu, Y. Xiong, S. X. Yu, and D. Lin, "Unsupervised feature learning via non-parametric instance discrimination," in *Proc. ICCV*, 2018, pp. 3733–3742.
- [22] T. Chen, S. Kornblith, M. Norouzi, and G. Hinton, "A simple framework for contrastive learning of visual representations," in *Proc. ICML*, PMLR, 2020, pp. 1597–1607.
- [23] J.-B. Grill, F. Strub, F. Alché, C. Tallec, P. Richemond, E. Buchatskaya, C. Doersch, B. Avila Pires, Z. Guo, M. Gheshlaghi Azar *et al.*, "Bootstrap your own latent—a new approach to self-supervised learning," *Advances in neural information processing systems*, vol. 33, pp. 21 271–21 284, 2020.
- [24] L. Jing and Y. Tian, "Self-supervised visual feature learning with deep neural networks: A survey," *IEEE transactions on pattern analysis and machine intelligence*, vol. 43, no. 11, pp. 4037–4058, 2020.
- [25] J. Zbontar, L. Jing, I. Misra, Y. LeCun, and S. Deny, "Barlow twins: Self-supervised learning via redundancy reduction," in *Proc. ICML*. PMLR, 2021, pp. 12 310–12 320.
- [26] T. Wang and P. Isola, "Understanding contrastive representation learning through alignment and uniformity on the hypersphere," in *Proc. ICML*. PMLR, 2020, pp. 9929–9939.
- [27] A. v. d. Oord, Y. Li, and O. Vinyals, "Representation learning with contrastive predictive coding," *arXiv preprint arXiv:1807.03748*, 2018.
- [28] Y. Li and S. Shan, "Contrastive learning of person-independent representations for facial action unit detection," *IEEE Transactions on Image Processing*, 2023.
- [29] P. H. Le-Khac, G. Healy, and A. F. Smeaton, "Contrastive representation learning: A framework and review," *Ieee Access*, vol. 8, pp. 193 907–193 934, 2020.
- [30] A. Jaiswal, A. R. Babu, M. Z. Zadeh, D. Banerjee, and F. Makedon, "A survey on contrastive self-supervised learning," *Technologies*, vol. 9, no. 1, p. 2, 2020.
- [31] M. Gutmann and A. Hyvärinen, "Noise-contrastive estimation: A new estimation principle for unnormalized statistical models," in *Proc. ICAIS*. JMLR Workshop and Conference Proceedings, 2010, pp. 297–304.
- [32] K. He, H. Fan, Y. Wu, S. Xie, and R. Girshick, "Momentum contrast for unsupervised visual representation learning," in *Proc. CVPR*, 2020, pp. 9729–9738.
- [33] M. Seyfi, A. Banitalebi-Dehkordi, and Y. Zhang, "Extending momentum contrast with cross similarity consistency regularization," *IEEE Transactions on Circuits and Systems for Video Technology*, vol. 32, no. 10, pp. 6714–6727, 2022.
- [34] W. Zhao, C. Li, W. Zhang, L. Yang, P. Zhuang, L. Li, K. Fan, and H. Yang, "Embedding global contrastive and local location in self-supervised learning," *IEEE Transactions on Circuits and Systems for Video Technology*, vol. 33, no. 5, pp. 2275–2289, 2022.
- [35] X. Chen and K. He, "Exploring simple siamese representation learning," in *Proc. CVPR*, 2021, pp. 15 750–15 758.
- [36] J. D. M.-W. C. Kenton and L. K. Toutanova, "Bert: Pre-training of deep bidirectional transformers for language understanding," in *Proc. NAACL*, vol. 1, 2019, p. 2.
- [37] A. Dosovitskiy, J. T. Springenberg, M. Riedmiller, and T. Brox, "Discriminative unsupervised feature learning with convolutional neural networks," *Advances in neural information processing systems*, vol. 27, 2014.
- [38] R. Devon Hjelm, A. Fedorov, S. Lavoie-Marchildon, K. Grewal, P. Bachman, A. Trischler, and Y. Bengio, "Learning deep representations by mutual information estimation and maximization," *arXiv e-prints*, pp. arXiv–1808, 2018.
- [39] S. Arora, H. Khandeparkar, M. Khodak, O. Plevrakis, and N. Saunshi, "A theoretical analysis of contrastive unsupervised representation learning," *arXiv preprint arXiv:1902.09229*, 2019.
- [40] P. Khosla, P. Teterwak, C. Wang, A. Sarna, Y. Tian, P. Isola, A. Maschinot, C. Liu, and D. Krishnan, "Supervised contrastive learning," *Advances in neural information processing systems*, vol. 33, pp. 18 661–18 673, 2020.
- [41] T. Chen, S. Kornblith, K. Swersky, M. Norouzi, and G. E. Hinton, "Big self-supervised models are strong semi-supervised learners," *Advances in neural information processing systems*, vol. 33, pp. 22 243–22 255, 2020.
- [42] X. Niu, H. Han, S. Shan, and X. Chen, "Multi-label co-regularization for semi-supervised facial action unit recognition," *Advances in neural information processing systems*, vol. 32, 2019.
- [43] X. Sun, J. Zeng, and S. Shan, "Emotion-aware contrastive learning for facial action unit detection," in *Proc. FG*. IEEE, 2021, pp. 01–08.
- [44] Y. Yang, Q. Hu, H. Lu, F. Jiang, and Y. Li, "Landmark-assisted facial action unit detection with optimal attention and contrastive learning," in *Proc. ICONIP*. Springer, 2023, pp. 92–104.
- [45] Z. Liu, R. Liu, Z. Shi, L. Liu, X. Mi, and K. Murase, "Semi-supervised contrastive learning with soft mask attention for facial action unit detection," in *Proc. ICASSP*. IEEE, 2023, pp. 1–5.
- [46] Y. Chang and S. Wang, "Knowledge-driven self-supervised representation learning for facial action unit recognition," in *Proc. CVPR*, 2022, pp. 20 417–20 426.
- [47] B.-F. Wu, Y.-T. Wei, B.-J. Wu, and C.-H. Lin, "Contrastive feature learning and class-weighted loss for facial action unit detection," in *Proc. SMC*. IEEE, 2019, pp. 2478–2483.
- [48] V. Suresh and D. C. Ong, "Using positive matching contrastive loss with facial action units to mitigate bias in facial expression recognition," in *Proc. ACII*. IEEE, 2022, pp. 1–8.
- [49] Y. Chen, C. Chen, X. Luo, J. Huang, X.-S. Hua, T. Wang, and Y. Liang, "Pursuing knowledge consistency: Supervised hierarchical contrastive learning for facial action unit recognition," in *Proc. ACM MM*, 2022, pp. 111–119.
- [50] Q. Kong, W. Wei, Z. Deng, T. Yoshinaga, and T. Murakami, "Cycle-contrast for self-supervised video representation learning," *Advances in Neural Information Processing Systems*, vol. 33, pp. 8089–8100, 2020.
- [51] A. Miech, J.-B. Alayrac, L. Smaira, I. Laptev, J. Sivic, and A. Zisserman, "End-to-end learning of visual representations from uncurated instructional videos," in *Proc. CVPR*, 2020, pp. 9879–9889.
- [52] Y. Li and G. Zhao, "Intra-and inter-contrastive learning for micro-expression action unit detection," in *Proc. ICMI*, 2021, pp. 702–706.
- [53] H. Wu and X. Wang, "Contrastive learning of image representations with cross-video cycle-consistency," in *Proc. ICCV*, 2021, pp. 10 149–10 159.
- [54] R. Qian, T. Meng, B. Gong, M.-H. Yang, H. Wang, S. Belongie, and Y. Cui, "Spatiotemporal contrastive video representation learning," in *Proc. CVPR*, 2021, pp. 6964–6974.
- [55] Y. Sun, J. Zeng, S. Shan, and X. Chen, "Cross-encoder for unsupervised gaze representation learning," in *Proc. ICCV*, 2021, pp. 3702–3711.
- [56] C. Luo, S. Song, W. Xie, L. Shen, and H. Gunes, "Learning multi-dimensional edge feature-based au relation graph for facial action unit recognition," *arXiv preprint arXiv:2205.01782*, 2022.
- [57] Z. Liu, Y. Lin, Y. Cao, H. Hu, Y. Wei, Z. Zhang, S. Lin, and B. Guo, "Swin transformer: Hierarchical vision transformer using shifted windows," in *Proc. ICCV*, 2021, pp. 10 012–10 022.
- [58] J. Robinson, C.-Y. Chuang, S. Sra, and S. Jegelka, "Contrastive learning with hard negative samples," *Proc. ICLR*, 2020.
- [59] F. Wang and H. Liu, "Understanding the behaviour of contrastive loss," in *Proc. CVPR*, June 2021, pp. 2495–2504.
- [60] D. Arpit, S. Jastrzkebski, N. Ballas, D. Krueger, E. Bengio, M. S. Kanwal, T. Maharaj, A. Fischer, A. Courville, Y. Bengio *et al.*, "A closer look at memorization in deep networks," in *Proc. ICML*, 2017, pp. 233–242.
- [61] C. Zhang, S. Bengio, M. Hardt, B. Recht, and O. Vinyals, "Understanding deep learning (still) requires rethinking generalization," *Communications of the ACM*, vol. 64, no. 3, pp. 107–115, 2021.
- [62] B. Han, Q. Yao, X. Yu, G. Niu, M. Xu, W. Hu, I. Tsang, and M. Sugiyama, "Co-teaching: Robust training of deep neural networks with extremely noisy labels," in *Proc. NeurIPS*, 2018, p. 31.
- [63] X. Zhang, L. Yin, J. F. Cohn, S. Canavan, M. Reale, A. Horowitz, P. Liu, and J. M. Girard, "Bp4d-spontaneous: a high-resolution spontaneous 3d dynamic facial expression database," *Image and Vision Computing*, vol. 32, no. 10, pp. 692–706, 2014.

- [64] S. M. Mavadati, M. H. Mahoor, K. Bartlett, P. Trinh, and J. F. Cohn, "Disfa: A spontaneous facial action intensity database," *IEEE Transactions on Affective Computing*, vol. 4, no. 2, pp. 151–160, 2013.
- [65] J. M. Girard, W.-S. Chu, L. A. Jeni, and J. F. Cohn, "Sayette group formation task (gft) spontaneous facial expression database," in *Proc. FG*. IEEE, 2017, pp. 581–588.
- [66] D. Kollias and S. Zafeiriou, "Expression, affect, action unit recognition: Aff-wild2, multi-task learning and arcfac," *arXiv preprint arXiv:1910.04855*, 2019.
- [67] X. Xiong and F. De la Torre, "Supervised descent method and its applications to face alignment," in *Proc. CVPR*, 2013, pp. 532–539.
- [68] T. F. Cootes, G. J. Edwards, and C. J. Taylor, "Active appearance models," *IEEE Transactions on pattern analysis and machine intelligence*, vol. 23, no. 6, pp. 681–685, 2001.
- [69] L. A. Jeni, J. F. Cohn, and T. Kanade, "Dense 3d face alignment from 2d video for real-time use," *Image and Vision Computing*, vol. 58, pp. 13–24, 2017.
- [70] D. E. King, "Dlib-ml: A machine learning toolkit," *The Journal of Machine Learning Research*, vol. 10, pp. 1755–1758, 2009.
- [71] V. Kazemi and J. Sullivan, "One millisecond face alignment with an ensemble of regression trees," in *Proc. CVPR*, 2014, pp. 1867–1874.
- [72] W. Zhang, Z. Guo, K. Chen, L. Li, Z. Zhang, Y. Ding, R. Wu, T. Lv, and C. Fan, "Prior aided streaming network for multi-task affective analysis," in *Proc. ICCV*, 2021, pp. 3539–3549.
- [73] R. Zhang, P. Isola, and A. A. Efros, "Colorful image colorization," in *Proc. ECCV*. Springer, 2016, pp. 649–666.
- [74] M. Noroozi and P. Favao, "Unsupervised learning of visual representations by solving jigsaw puzzles," in *Proc. ECCV*. Springer, 2016, pp. 69–84.
- [75] Y. Li and S. Shan, "Meta auxiliary learning for facial action unit detection," *IEEE Transactions on Affective Computing*, 2023.
- [76] Z. Shang, C. Du, B. Li, Z. Yan, and L. Yu, "Mma-net: Multi-view mixed attention mechanism for facial action unit detection," *Pattern Recognition Letters*, 2023.
- [77] H. Yang, L. Yin, Y. Zhou, and J. Gu, "Exploiting semantic embedding and visual feature for facial action unit detection," in *Proc. CVPR*, 2021, pp. 10482–10491.
- [78] T. Song, Z. Cui, W. Zheng, and Q. Ji, "Hybrid message passing with performance-driven structures for facial action unit detection," in *Proc. CVPR*, 2021, pp. 6267–6276.
- [79] Z. Shao, Y. Zhou, J. Cai, H. Zhu, and R. Yao, "Facial action unit detection via adaptive attention and relation," *IEEE Transactions on Image Processing*, 2023.
- [80] Z. Li, X. Deng, X. Li, and L. Yin, "Integrating semantic and temporal relationships in facial action unit detection," in *Proc. ACM MM*, 2021, pp. 5519–5527.
- [81] Z. Cui, C. Kuang, T. Gao, K. Talamadupula, and Q. Ji, "Biomechanics-guided facial action unit detection through force modeling," in *Proc. CVPR*, 2023, pp. 8694–8703.
- [82] X. Zhang, T. Wang, X. Li, H. Yang, and L. Yin, "Weakly-supervised text-driven contrastive learning for facial behavior understanding," in *Proc. ICCV*, 2023, pp. 20751–20762.
- [83] A. Krizhevsky, I. Sutskever, and G. E. Hinton, "Imagenet classification with deep convolutional neural networks," *Proc. NIPS*, vol. 25, 2012.
- [84] R.-E. Fan, K.-W. Chang, C.-J. Hsieh, X.-R. Wang, and C.-J. Lin, "Liblinear: A library for large linear classification," *the Journal of machine Learning research*, vol. 9, pp. 1871–1874, 2008.
- [85] Y. Li, J. Zeng, S. Shan, and X. Chen, "Self-supervised representation learning from videos for facial action unit detection," in *Proc. CVPR*, 2019, pp. 10924–10933.
- [86] I. O. Ertugrul, J. F. Cohn, L. A. Jeni, Z. Zhang, L. Yin, and Q. Ji, "Crossing domains for au coding: Perspectives, approaches, and measures," *IEEE transactions on biometrics, behavior, and identity science*, vol. 2, no. 2, pp. 158–171, 2020.
- [87] Y. Li, J. Zeng, and S. Shan, "Learning representations for facial actions from unlabeled videos," *IEEE Transactions on Pattern Analysis and Machine Intelligence*, vol. 44, no. 1, pp. 302–317, 2022.
- [88] K. He, X. Zhang, S. Ren, and J. Sun, "Deep residual learning for image recognition," in *Proc. CVPR*, 2016, pp. 770–778.
- [89] W. Huang, M. Yi, X. Zhao, and Z. Jiang, "Towards the generalization of contrastive self-supervised learning," *Proc. ICLR*, 2023.
- [90] S. Joshi and B. Mirzasoleiman, "Data-efficient contrastive self-supervised learning: Most beneficial examples for supervised learning contribute the least," in *Proc. ICML*. PMLR, 2023, pp. 15356–15370.



Ziqiao Shang received the B.Eng. degree in information engineering from the Wuhan University of Technology, Wuhan, China, in 2021. He is currently pursuing the M.Sc. degree with the School of Electronic Information and Communications, Huazhong University of Science and Technology, Wuhan, China. His research interests mainly include facial related computer vision tasks, such as facial action unit detection and micro-expression recognition.



Bin Liu received the Ph.D. degree from School of Electronic Information and Communications, Huazhong University of Science and Technology, Wuhan, China, in 2023. He is working as a post-doctoral fellow with the School of Computing and Artificial Intelligence, Southwest Jiaotong University, Chengdu, China. His research interests include artificial intelligence and machine learning.



Fengmao Lv received the bachelor's and Ph.D. degrees in computer science from the University of Electronic Science and Technology of China, Chengdu, China, in 2013 and 2018, respectively. He is currently an Associate Professor with Southwest Jiaotong University, Chengdu. His current research interests include transfer learning, domain adaptation, and their applications in computer vision and natural language processing.



Fei Teng (Member, IEEE) received the BS degree from Southwest Jiaotong University, Chengdu, China, in 2006, and the PhD degree in computer science and technology from Ecole Centrale deParis, Paris, France, in 2011. She is currently an associate professor with the School of Computing and Artificial Intelligence, Southwest Jiaotong University. Her research interests include medical informatics and data mining.



Tianrui Li (Senior Member, IEEE) received the BS, MS, and PhD degrees from Southwest Jiaotong University, Chengdu, China, in 1992, 1995, and 2002, respectively. He is currently a professor with the School of Computing and Artificial Intelligence, Southwest Jiaotong University. His research interests include data mining and knowledge engineering.